Second-order coherence of superradiance from a Bose-Einstein condensate

R. Lopes, A. Imanaliev, M. Bonneau,* J. Ruaudel,† M. Cheneau, D. Boiron, and C. I. Westbrook‡
Laboratoire Charles Fabry, Institut d'Optique–CNRS–Université Paris-Sud, 2 avenue Augustin Fresnel, 91127 Palaiseau, France
(Received 23 December 2013; published 16 July 2014)

We have measured the two-particle correlation function of atoms from a Bose-Einstein condensate participating in a superradiance process, which directly reflects the second-order coherence of the emitted light. We compare this correlation function with that of atoms undergoing stimulated emission. Whereas the stimulated process produces correlations resembling those of a coherent state, we find that superradiance, even in the presence of strong gain, shows a correlation function close to that of a thermal state, just as for ordinary spontaneous emission.

DOI: 10.1103/PhysRevA.90.013615 PACS number(s): 03.75.Kk, 42.50.Lc, 67.10.Jn

Ever since the publication of Dicke's 1954 paper [1], the problem of the collective emission of radiation has occupied many researchers in the fields of light scattering, lasers, and quantum optics. Collective emission is characterized by a rate of emission which is strongly modified compared to that of individual atoms [2]. It occurs in many different contexts: hot gases, cold gases, solids and even planetary and astrophysical environments [3]. The case of an enhanced rate of emission, originally dubbed superradiance, is closely connected to stimulated emission and gain and, as such, resembles laser emission [4]. Lasers are typically characterized by high phase coherence but also by a stable intensity, corresponding to a Poissonian noise, or a flat second-order correlation function [5]. Here we present measurements showing that the coherence properties of superradiance, when it occurs in an ultracold gas and despite strong amplified emission, are much closer to those of a thermal state, with super-Poissonian-intensity noise.

Research has shown that the details of collective emission depend on many parameters such as the pumping configuration, dephasing and relaxation processes, sample geometry, presence of a cavity, etc., and, as a result, a complex nomenclature has evolved including the terms superradiance, superfluorescence, amplified spontaneous emission, mirrorless lasing, and random lasing [2,4,6–9], the distinctions among which we do not attempt to summarize here. The problem has recently seen renewed interest in the field of cold atoms [10–25]. This is partly because cold atoms provide a reproducible, easily characterized ensemble in which Doppler broadening effects are small and relaxation is generally limited to spontaneous emission. Most cold-atom experiments differ in an important way from the archetypal situation first envisioned by Dicke: instead of creating an ensemble of excited atoms at a well-defined time and then allowing this ensemble to evolve freely, the sample is typically pumped during a period long compared to the relaxation time and emission lasts essentially only as long as the pumping. The authors of Ref. [10], however, have argued that there is a close analogy to the Dicke problem, and we follow them in designating this process superradiance.

In the literature on superradiance there has been relatively little discussion about the coherence and correlation properties of the light. The theoretical treatments we are aware of show that the coherence of collective emission can be quite complicated but does not resemble that of a laser [2,13,20,26–28]. These results, however, were obtained for simple models that do not include all parameters relevant to laboratory experiments. Experimentally, a study performed on Rydberg atoms coupled to a millimeter-wave cavity [29] showed a thermal mode occupation, and an experiment in a cold atomic vapor in free space [24] observed a nonflat second-order correlation function. In the present work, we show that even if the initial atomic state is a Bose-Einstein condensate (BEC), the second-order correlation function looks thermal rather than coherent.

Such behavior, which may seem counterintuitive, can be understood by describing superradiance as a four-wave mixing process between two matter waves and two electromagnetic waves. The initial state consists of a condensate, a coherent optical pump beam, and empty modes for the scattered atoms and the scattered photons. If we make the approximation that the condensate and the pump beam are not depleted and can be treated as classical fields, the matter-radiation interaction Hamiltonian is given by

$$\hat{H} = \sum_i [\chi_i \, \hat{a}^\dagger_{\mathrm{at},i} \, \hat{a}^\dagger_{\mathrm{ph},i} + \chi_i^* \, \hat{a}_{\mathrm{at},i} \, \hat{a}_{\mathrm{ph},i}], \tag{1}$$

where $\hat{a}^\dagger_{\mathrm{at},i}$ ($\hat{a}_{\mathrm{at},i}$) and $\hat{a}^\dagger_{\mathrm{ph},i}$ ($\hat{a}_{\mathrm{ph},i}$) denote atom and photon creation (annihilation) operators for a specific pair of momenta i fixed by energy and momentum conservation and χ_i is a coupling constant. Textbooks [30] show that, starting from an input vacuum state, this Hamiltonian leads to a product of two-mode squeezed states. When one traces over one of the two modes, $\alpha = \{\mathrm{at},i\}$ or $\{\mathrm{ph},i\}$, the remaining mode β has a thermal occupation with a normalized two-particle or second-order correlator

$$\frac{\langle \hat{a}^\dagger_\beta \, \hat{a}^\dagger_\beta \, \hat{a}_\beta \, \hat{a}_\beta \rangle}{\langle \hat{a}^\dagger_\beta \, \hat{a}_\beta \rangle^2} = 2, \tag{2}$$

whereas it is unity for a laser. The problem has also been treated for four-wave mixing of matter waves [31]. We emphasize

*Current address: Vienna Center for Quantum Science and Technology, Atominstitut, TU Wien, Stadionallee 2, 1020 Vienna, Austria.
†Current address: Laboratoire Kastler Brossel, Université Pierre et Marie Curie–École normale supérieure–CNRS, 4 place Jussieu, 75005 Paris, France.
‡christoph.westbrook@institutoptique.fr

that, when starting from initially empty modes, the occupation remains thermal *regardless* of the gain.

In the experiment, we start from initially nearly motionless atoms of a BEC and observe their recoil upon photon emission. To the extent that each recoil corresponds to the emission of a single photon, we can obtain essentially the same information about the radiation from such measurements as by observing it directly. In doing this, we are following the approach pioneered in experiments such as [10] and [29] and followed by many others, which uses highly developed atom detection and imaging techniques to glean most of the experimental information about the process. We are able to make time-integrated measurements of the emission, resolved in transverse and longitudinal momentum as well as in polarization, and reconstruct the two-particle correlation function of the recoiling atoms or, equivalently, the second-order correlation function of the scattered light. We show that in the configuration of our experiment, the second-order correlation is close to that of a thermal sample and very different from the correlation properties of the initial, condensed atomic state.

We use helium in the $2\,^3S_1$, $m = 1$ state confined in a crossed dipole trap [see Fig. 1(a)] with frequencies of 1300 Hz in the x and y directions and 130 Hz in the (vertical) z direction. The dipole trap wavelength is 1.5 μm. The atom number is approximately 50 000, and the temperature of the remaining thermal cloud 140 nK. A 9-G magnetic field along the y axis defines a quantization axis. After producing the condensate, we irradiate it with a laser pulse of 2.4 W/cm^2 tuned 600 MHz to the red of the $2\,^3S_1 \rightarrow 2\,^3P_0$ transition at $\lambda = 1083$ nm and with natural linewidth 1.6 MHz. The excitation beam propagates

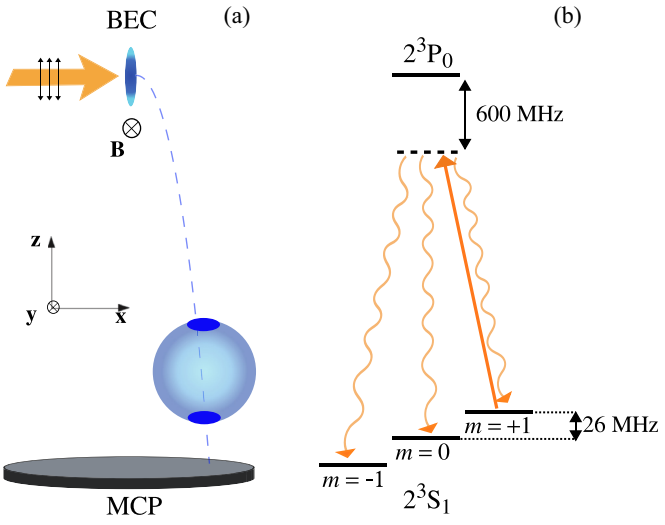

FIG. 1. (Color online) (a) Sketch of the experiment. A 9-G magnetic field **B** applied along the y axis defines the quantization axis. The excitation beam propagates with an angle of 10° (not shown) relative to the x axis and its polarization is linear, with the same angle relative to the z axis. After emission, the atoms fall 46 cm to a position-sensitive microchannel plate (MCP). The atom cloud forms a sphere with enhanced occupation of the endfire modes. (b) Atomic level scheme. The atoms, initially in the $2\,^3S_1$, $m = +1$ state, are excited to the $2\,^3P_0$ state. From there, they can decay with equal branching ratios to the three sublevels of the ground state. We detect only the atoms which scatter into the $m = 0$ state.

with an angle of 10° relative to the x axis and its polarization is linear, with the same angle relative to the z axis [see Fig. 1(a)]. The pulse length is 5 μs and it is applied with a delay τ after switching off the trap. The expansion of the cloud during this delay is a convenient way to vary both the optical density and the anisotropy of the sample at constant atom number. The absorption dipole matrix element is of the σ^- form and thus one-half of the laser intensity is coupled to the atomic transition corresponding to a Rabi frequency of 56 MHz. The excited atoms decay with equal branching ratios to the three ground states. During the pulse, less than 10% of the atoms are pumped into each of these states. Because of the polarization selection rules, the atoms which are pumped into the $m = 0$ state cannot reabsorb light from the excitation laser. By focusing on these atoms, we study the regime of "Raman superradiance" [15,32], by which we mean that an absorption and emission cycle is accompanied by a change in the internal state of the atom. When the trap is switched off, the atoms fall toward a microchannel plate detector which detects individual atoms with three-dimensional imaging capability and a 10% to 20% quantum efficiency [33]. A magnetic-field gradient is applied to sweep away all atoms except those scattered into the $m = 0$ magnetic sublevel. The average time of flight to the detector is 310 ms and is long enough that the atoms' positions at the detector reflect the atomic momenta after interaction with the excitation laser. Conservation of momentum then requires that these atoms lie on a sphere with a radius equal to the recoil momentum $k_{\rm rec} = 2\pi/\lambda$. Any additional scattering of light, whether from imperfect polarization of the excitation laser or from multiple scattering by the atoms, will result in the atoms lying outside the sphere. We see no significant signal from such events, but in order to completely eliminate the possibility of multiple scattering we restrict our analysis of the data to the spherical shell with inner radius $0.8\,k_{\rm rec}$ and outer radius $1.2\,k_{\rm rec}$.

We excite atoms in an elongated BEC in such a way that an allowed emission dipole can radiate along the long axis. In an anisotropic source, collective emission builds up more efficiently in the directions of highest optical thickness. Superradiance is therefore expected to occur along the long axis of the BEC, in so-called "endfire" modes [10,34]. An important parameter, then, is the Fresnel number of the sample [2], $F = 2R_\perp^2/\lambda R_z$, where $R_\perp$ and R_z are the horizontal and vertical Thomas-Fermi radii of the condensate. The Fresnel number distinguishes between the diffraction limited ($F < 1$) and the multimode superradiance regimes ($F > 1$). In our case, $R_\perp \approx 5$ μm and $R_z \approx 50$ μm, yielding a Fresnel number of about unity.

Typical cuts through the atomic momentum distribution in the yz plane are shown in Fig. 2, for $\tau = 500$ μs (left) and $\tau \approx 0$ (right). In both cases, the spherical shell with radius $1\,k_{\rm rec}$ appears clearly. For the short delay, when the atomic sample remains dense and anisotropic, we observe strong scattering in the endfire modes at the top and bottom poles of the sphere. In addition to this change in the profile of the distribution, we measure an increase in the *total number* of atoms on the sphere by a factor of ~5 from $\tau = 500$ μs to $\tau \approx 0$. Because each atom has scattered a single photon, this increase directly reflects an increase in the rate of emission in the sample and therefore demonstrates the collective nature

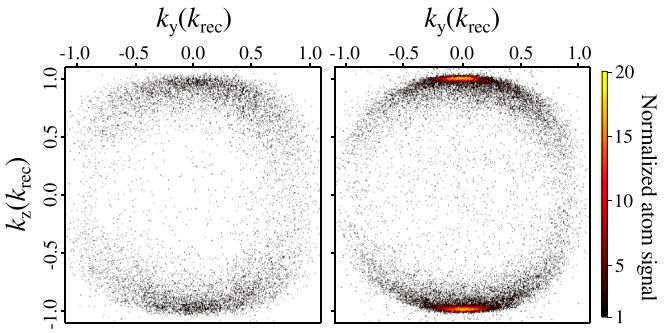

FIG. 2. (Color online) Momentum distribution of scattered atoms in the yz plane (containing the emission dipole). Both panels show the distribution in the yz plane, integrated between $k_x = \pm 0.1\, k_{rec}$ and summed over 100 shots. See the Supplemental Information for a cut in the xz plane [35]. Left: Excitation laser applied 500 μs after the trap switch-off. Only the radiation pattern for a y-polarized dipole is visible. Right: Excitation laser applied immediately after the trap switch-off. Strong superradiance is visible in the vertical, endfire modes.

of the scattering process. At long delays, the condensate has expanded sufficiently that the optical thickness and anisotropy have fallen dramatically, suppressing the collective scattering. By looking at the number of scattered atoms in the x direction (perpendicular to the plane in Fig. 2), we have verified that, away from the endfire modes, the rate of emission varies by less than 10% for different delays [35].

To see the distribution in a more quantitative way, we show in Fig. 3 an angular plot of the atom distribution in the yz plane. Data are shown for three delays τ before application of the

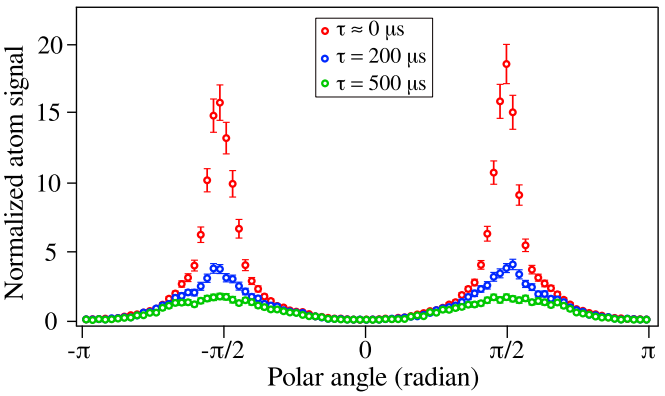

FIG. 3. (Color online) Angular distribution of scattered atoms in the yz plane (containing the emission dipole) for different values of the delay τ before the excitation pulse. From bottom to top: light-gray (green) circles correspond to $\tau = 500$ μs; dark-gray (blue) circles, to $\tau = 200$ μs; and light-gray (red) circles, to $\tau = 0$ μs. Data for $\tau = 0$ and 500 μs are the same as those shown in Fig. 2. Images were integrated along the x axis between $\pm 0.1\, k_{rec}$, and only atoms lying inside a shell with inner radius $0.8\, k_{rec}$ and outer radius $1.2\, k_{rec}$ were taken into account. The delays $\tau = 0$, 200, and 500 μs correspond to peak densities of $\approx$8, 2, and 0.4×10^{18} m^{-3} and to aspect ratios of 10, 5, and 2.5, respectively. The endfire modes are located at $\pm\pi/2$. The half-width at half-maximum of the highest peak is 0.14 rad. Error bars are shown, denoting the 68% confidence interval.

excitation pulse. For the 500-μs delay, the angular distribution follows the well-known "$\sin^2\theta$" linear dipole emission pattern, with the angles $\theta = 0$ and π corresponding to the orientation of the dipole along the y axis [35]. For the 200-μs delay, the superradiant peaks are already visible at the top of the dipole emission profile. For the shortest delay, the half-width of the superradiant peaks is $0.14\, k_{rec}$, or 0.14 rad, consistent with the diffraction angle and the aspect ratio of the source. In the vertical direction, the superradiant peaks are 10 times narrower than in the horizontal direction [35].

In the strongly superradiant case, we observe large and uncorrelated fluctuations of the heights of the two superradiant peaks on a shot-to-shot basis. These fluctuations directly reflect the fluctuations of the population of the superradiant modes. We investigate these fluctuations further by measuring the normalized two-particle correlation function of the scattered atoms, defined as

$$g^{(2)}(\Delta\mathbf{k}) = \frac{\langle : \hat{n}(\mathbf{k})\hat{n}(\mathbf{k}+\Delta\mathbf{k}) : \rangle}{\langle \hat{n}(\mathbf{k})\rangle\ \langle \hat{n}(\mathbf{k}+\Delta\mathbf{k})\rangle}. \tag{3}$$

Here, $\hat{n}$ is the atomic density and : : denotes normal ordering. In practice, this function is obtained from a histogram of pair separations $\Delta\mathbf{k}$ normalized to the autoconvolution of the average particle momentum distribution [36,37]. Figure 4 shows the experimentally measured correlation functions integrated over the momentum along two of three axes, both

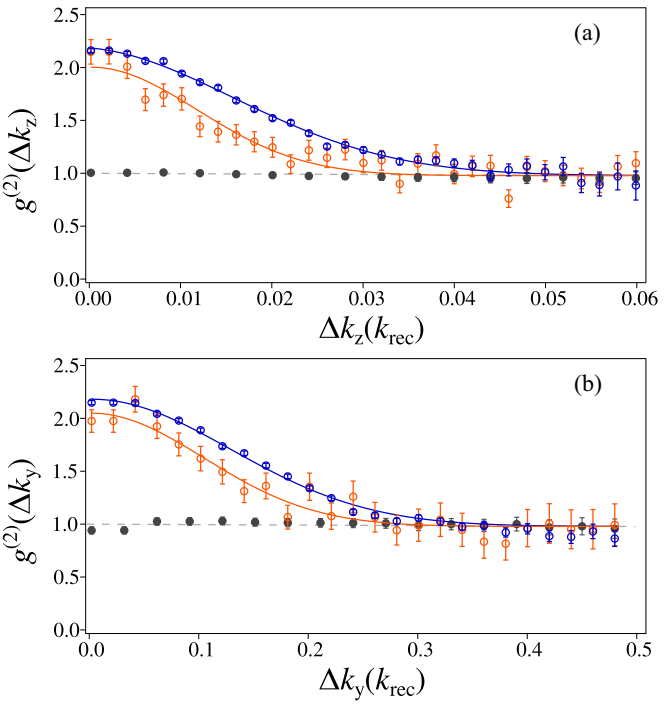

FIG. 4. (Color online) Correlation functions along the (a) z and (b) y axis for $\tau \approx 0$. Darker (blue) circles correspond to superradiant peaks (defined by $|k_z| > 0.95\, k_{rec}$). Lighter (orange) circles correspond to atoms from the scattering sphere away from the superradiant peaks (defined by $|k_z| < 0.92\, k_{rec}$). Solid lines are Gaussian fits constrained to approach unity at large separation. Filled gray circles correspond to a fraction of the initial condensate transferred to the $m = 0$ state via a stimulated Raman transfer. The dashed gray line shows unity. Error bars denote the 68% confidence interval.

for the superradiant peaks and on the scattering sphere away from the peaks [35].

We see that in both cases the correlation function at zero separation reaches a value close to 2. This shows clearly that, despite strong amplified emission in the endfire modes, the atoms undergoing a superradiant process have statistics comparable to that of a thermal sample. As emphasized in the introductory section, these large fluctuations can be simply understood by modeling the superradiant emission as a four-wave mixing process; they arise from the fact that the emission is triggered by spontaneous emission. For the superradiant peaks, the correlation actually is slightly larger than 2. Similar behavior has appeared in some models [20,38], but these models may not be directly applicable to our situation.

Figure 4 also shows that the correlation widths of the superradiant modes are somewhat broader than those of the atoms scattered in other modes. The effect is a factor of about 1.5 in the vertical direction and about 1.25 in the horizontal direction [35]. The broadening indicates that the effective source size for superradiance is slightly smaller than that for spontaneous scattering. A decreased vertical source size for superradiance is consistent with the observations in Refs. [39] and [40], which showed that the superradiant emission is concentrated near the ends of the sample. In the horizontal direction, one also expects a slightly reduced source size relative to the atom cloud since the gain is higher in the center, where the density is higher. The fact that the correlation widths are close to the widths of the momentum distribution [35] indicates that the superradiant peaks are almost single mode as expected for samples with a Fresnel number close to unity [2].

The spontaneous superradiant scattering process should be contrasted with stimulated Raman scattering. In terms of the model described by Hamiltonian (1), stimulated Raman scattering corresponds to seeding one of the photon modes with a coherent state. In this case, vacuum fluctuations do not initiate the scattering process, and the resulting mode occupation is not thermal but coherent. To study stimulated scattering, we applied the excitation beam together with another beam polarized parallel to the magnetic field and detuned by the Zeeman shift (25 MHz) with respect to the σ-polarized beam, inducing a stimulated Raman transition. The laser intensities were adjusted to transfer a similar number of atoms to the $m = 0$ state as in the superradiance experiment. The normalized correlation functions in this situation, shown in Fig. 4, are very nearly flat and equal to unity as we expect for a BEC [36,41,42]. The complementary experiment, seeding the *atomic* mode with a coherent state has also been observed to produce a coherent amplified matter wave [43,44]. As a side remark, we have also observed that the superradiant atom peaks are 2.8 times narrower in the vertical direction than the vertical width of the transferred condensate [35]. We attribute this to a longitudinal gain narrowing effect [27].

We also investigated the influence of several other experimental parameters on the second-order coherence of the superradiant emission: We have excited the atomic sample with a longer and stronger pulse (10 μs, 3.2 W/cm^2), so that the initial condensate was entirely depleted. We have explored the Rayleigh scattering regime, in which the atoms scatter back to their initial internal state. We also changed the longitudinal confinement frequency of the BEC to 7 Hz, leading to a much higher aspect ratio. These different configurations led to two-particle correlation functions which were very similar to the one discussed above. We believe that similar fluctuations will occur in superradiance from a thermal cloud provided that the gain in the medium is large enough. We were unable to confirm this experimentally in our system, precisely because of the vastly reduced optical density. However, noncoherent intensity fluctuations have been observed using magneto-optically trapped atoms [24]. This seems to confirm our interpretation that the large fluctuations of the superradiant mode occupation is an intrinsic property of superradiant emission, reflecting the seeding by spontaneous emission. The only way to suppress these fluctuations would be to restrict the number of scattering modes to one by means of a cavity and to saturate the gain by completely depleting the atomic cloud. The occupation of the superradiant mode would then simply reflect that of the initial atomic sample.

An interesting extension of the techniques used here is to examine superradiant Rayleigh scattering of a light pulse short enough and strong enough to populate oppositely directed modes [45]. It has been predicted [13,14,46] that the modes propagating in opposite directions are entangled, similar to those produced in atomic four-wave mixing [47–49]. A similar measurement technique should be able to reveal them.

We acknowledge fruitful discussions with A. Browaeys, J.-J. Greffet, and P. Pillet. This work was supported by the IFRAF institute, the Triangle de la Physique, the LABEX PALM, the ANR-ProQuP project, and the ERC Quantatop (Grant No. 267 775). J.R. was supported by the DGA; R.L., by FCT scholarship SFRH/BD/74352/2010.

[1] R. H. Dicke, Phys. Rev. **93**, 99 (1954).
[2] M. Gross and S. Haroche, Phys. Rep. **93**, 301 (1982).
[3] V. Letokhov and S. Johansson, *Astrophysical Lasers* (Oxford University Press, New York, 2008).
[4] A. E. Siegman, *Lasers* (University Science Books, Mill Valley, CA, 1986).
[5] R. Loudon, *The Quantum Theory of Light* (Oxford University Press, Oxford, 2000).
[6] N. Rehler and J. Eberly, Phys. Rev. A **3**, 1735 (1971).
[7] L. Allen and G. Peters, Phys. Rev. A **8**, 2031 (1973).
[8] R. Bonifacio and L. Lugiato, Phys. Rev. A **11**, 1507 (1975).
[9] J. MacGillivray and M. Feld, Phys. Rev. A **14**, 1169 (1976).
[10] S. Inouye, A. P. Chikkatur, D. M. Stamper-Kurn, J. Stenger, D. E. Pritchard, and W. Ketterle, Science **285**, 571 (1999).
[11] M. G. Moore, O. Zobay, and P. Meystre, Phys. Rev. A **60**, 1491 (1999).
[12] Ö. E. Müstecaplioglu and L. You, Phys. Rev. A **62**, 063615 (2000).
[13] N. Piovella, M. Cola, and R. Bonifacio, Phys. Rev. A **67**, 013817 (2003).

[14] H. Pu, W. Zhang, and P. Meystre, Phys. Rev. Lett. **91**, 150407 (2003).
[15] Y. Yoshikawa, T. Sugiura, Y. Torii, and T. Kuga, Phys. Rev. A **69**, 041603 (2004).
[16] N. Bar-Gill, E. E. Rowen, and N. Davidson, Phys. Rev. A **76**, 043603 (2007).
[17] T. Wang, S. F. Yelin, R. Côté, E. E. Eyler, S. M. Farooqi, P. L. Gould, M. Koštrun, D. Tong, and D. Vrinceanu, Phys. Rev. A **75**, 033802 (2007).
[18] E. Paradis, B. Barrett, A. Kumarakrishnan, R. Zhang, and G. Raithel, Phys. Rev. A **77**, 043419 (2008).
[19] A. Hilliard, F. Kaminski, R. le Targat, C. Olausson, E. S. Polzik, and J. H. Müller, Phys. Rev. A **78**, 051403 (2008).
[20] D. Meiser and M. J. Holland, Phys. Rev. A **81**, 063827 (2010).
[21] L. Deng, E. W. Hagley, Q. Cao, X. Wang, X. Luo, R. Wang, M. G. Payne, F. Yang, X. Zhou, X. Chen *et al.*, Phys. Rev. Lett. **105**, 220404 (2010).
[22] T. Vogt, B. Lu, X. X. Liu, X. Xu, X. Zhou, and X. Chen, Phys. Rev. A **83**, 053603 (2011).
[23] J. G. Bohnet, Z. Chen, J. M. Weiner, D. Meiser, M. J. Holland, and J. K. Thompson, Nature **484**, 78 (2012).
[24] J. A. Greenberg and D. J. Gauthier, Phys. Rev. A **86**, 013823 (2012).
[25] Q. Baudouin, N. Mercadier, V. Guarrera, W. Guerin, and R. Kaiser, Nat. Phys. **9**, 357 (2013).
[26] F. Haake and R. J. Glauber, Phys. Rev. A **5**, 1457 (1972).
[27] M. G. Moore and P. Meystre, Phys. Rev. Lett. **83**, 5202 (1999).
[28] V. V. Temnov and U. Woggon, Opt. Express **17**, 5774 (2009).
[29] J.-M. Raimond, P. Goy, M. Gross, C. Fabre, and S. Haroche, Phys. Rev. Lett. **49**, 1924 (1982).
[30] C. C. Gerry and P. Knight, *Introductory Quantum Optics* (Cambridge University Press, Cambridge, 2005).
[31] K. Mølmer, A. Perrin, V. Krachmalnicoff, V. Leung, D. Boiron, A. Aspect, and C. I. Westbrook, Phys. Rev. A **77**, 033601 (2008).
[32] D. Schneble, G. K. Campbell, E. W. Streed, M. Boyd, D. E. Pritchard, and W. Ketterle, Phys. Rev. A **69**, 041601 (2004).
[33] J.-C. Jaskula, M. Bonneau, G. B. Partridge, V. Krachmalnicoff, P. Deuar, K. V. Kheruntsyan, A. Aspect, D. Boiron, and C. I. Westbrook, Phys. Rev. Lett. **105**, 190402 (2010).
[34] R. H. Dicke, in *Quantum Electronics; Proceedings of the Third International Congress, Paris.*, edited by P. Grivet and N. Bloembergen (Columbia University Press, New York, 1964).
[35] See Supplemental Material at http://link.aps.org/supplemental/10.1103/PhysRevA.90.013615 for the atomic distribution in the xz plane, details on the calculation of the correlation functions, and a table summarizing the widths of the momentum distributions and correlation functions.
[36] M. Schellekens, R. Hoppeler, A. Perrin, J. V. Gomes, D. Boiron, A. Aspect, and C. I. Westbrook, Science **310**, 648 (2005).
[37] K. V. Kheruntsyan, J.-C. Jaskula, P. Deuar, M. Bonneau, G. B. Partridge, J. Ruaudel, R. Lopes, D. Boiron, and C. I. Westbrook, Phys. Rev. Lett. **108**, 260401 (2012).
[38] T. Wasak, J. Chwedeńczuk, P. Ziń, and M. Trippenbach, Phys. Rev. A **86**, 043621 (2012).
[39] O. Zobay and G. M. Nikolopoulos, Phys. Rev. A **73**, 013620 (2006).
[40] L. E. Sadler, J. M. Higbie, S. R. Leslie, M. Vengalattore, and D. M. Stamper-Kurn, Phys. Rev. Lett. **98**, 110401 (2007).
[41] A. Öttl, S. Ritter, M. Köhl, and T. Esslinger, Phys. Rev. Lett. **95**, 090404 (2005).
[42] S. S. Hodgman, R. G. Dall, A. G. Manning, K. G. H. Baldwin, and A. G. Truscott, Science **331**, 1046 (2011).
[43] S. Inouye, T. Pfau, S. Gupta, A. P. Chikkatur, A. Gorlitz, D. E. Pritchard, and W. Ketterle, Nature **402**, 641 (1999).
[44] M. Kozuma, Y. Suzuki, Y. Torii, T. Sugiura, T. Kuga, E. Hagley, and L. Deng, Science **286**, 2309 (1999).
[45] D. Schneble, Y. Torii, M. Boyd, E. W. Streed, D. E. Pritchard, and W. Ketterle, Science **300**, 475 (2003).
[46] L. F. Buchmann, G. M. Nikolopoulos, O. Zobay, and P. Lambropoulos, Phys. Rev. A **81**, 031606 (2010).
[47] W. RuGway, S. S. Hodgman, R. G. Dall, M. T. Johnsson, and A. G. Truscott, Phys. Rev. Lett. **107**, 075301 (2011).
[48] R. Bucker, J. Grond, S. Manz, T. Berrada, T. Betz, C. Koller, U. Hohenester, T. Schumm, A. Perrin, and J. Schmiedmayer, Nat. Phys. **7**, 608 (2011).
[49] M. Bonneau, J. Ruaudel, R. Lopes, J.-C. Jaskula, A. Aspect, D. Boiron, and C. I. Westbrook, Phys. Rev. A **87**, 061603 (2013).